2013

# Conducting carbon nanofibre networks: dispersion optimisation, evaporative casting and direct writing

Holly Warren
*University of Wollongong*, hwarren@uow.edu.au

Reece D. Gately
*University of Wollongong*, rdg604@uowmail.edu.au

Hayley N. Moffat
*University of Wollongong*, hm547@uowmail.edu.au

Marc in het Panhuis
*University of Wollongong*, panhuis@uow.edu.au

## Publication Details

Warren, H., Gately, R. D., Moffat, H. N. & in het Panhuis, M. (2013). Conducting carbon nanofibre networks: dispersion optimisation, evaporative casting and direct writing. RSC Advances, 3 (44), 21936-21942.

# Conducting carbon nanofibre networks: dispersion optimisation, evaporative casting and direct writing

**Abstract**
The optimisation of vapour-grown carbon nanofibres (VGCNFs) dispersed in the biopolymer gellan gum (GG) and its usage as an ink for the direct writing of conducting networks are reported. Sonication optimisation showed that dispersing 10 mg per mL VGCNFs required 3 mg per mL GG solution and 4 minutes of low energy probe sonication. Free-standing films prepared by evaporative casting were found to exhibit electrical conductivity values of up to 35 ± 2 S cm-1. It is demonstrated that sonolysis has a detrimental effect on electrical conductivity. The dispersions were easily modified to allow for direct writing of conducting networks on paper using a commercial fountain pen. The electrical characteristics of these direct written electrodes (on paper) improved with increasing number of layers. The written electrodes on paper were used to connect a battery to a light emitting diode to demonstrate that they can be used in simple devices.

**Keywords**
evaporative, optimisation, dispersion, direct, networks, casting, nanofibre, carbon, conducting, writing



**Publication Details**
Warren, H., Gately, R. D., Moffat, H. N. & in het Panhuis, M. (2013). Conducting carbon nanofibre networks: dispersion optimisation, evaporative casting and direct writing. RSC Advances, 3 (44), 21936-21942.

RSC Advances

RSC Publishing

PAPER

View Article Online
View Journal | View Issue



Cite this: *RSC Adv.*, 2013, **3**, 21936

# Conducting carbon nanofibre networks: dispersion optimisation, evaporative casting and direct writing†

Holly Warren,[a] Reece D. Gately,[a] Hayley N. Moffat[a] and Marc in het Panhuis*[ab]

Received 19th July 2013
Accepted 13th September 2013

DOI: 10.1039/c3ra43743d

**www.rsc.org/advances**

The optimisation of vapour-grown carbon nanofibres (VGCNFs) dispersed in the biopolymer gellan gum (GG) and its usage as an ink for the direct writing of conducting networks are reported. Sonication optimisation showed that dispersing 10 mg per mL VGCNFs required 3 mg per mL GG solution and 4 minutes of low energy probe sonication. Free-standing films prepared by evaporative casting were found to exhibit electrical conductivity values of up to 35 ± 2 S $cm^{-1}$. It is demonstrated that sonolysis has a detrimental effect on electrical conductivity. The dispersions were easily modified to allow for direct writing of conducting networks on paper using a commercial fountain pen. The electrical characteristics of these direct written electrodes (on paper) improved with increasing number of layers. The written electrodes on paper were used to connect a battery to a light emitting diode to demonstrate that they can be used in simple devices.

## 1. Introduction

Additive manufacturing or rapid prototyping refers to techniques capable of building structures layer-by-layer, such as 3D printing,[1] laser sintering,[2] air-brush spraying,[3] dip-pen nanolithography,[4] slot-dye coating,[5] gravure printing,[6] inkjet printing[7–9] and extrusion printing.[10] These techniques have been extensively used for the fabrication of conductive electronics. Recently, conducting paper substrates have been used as part of low-cost, flexible, disposable devices.[11–13] This has led to the emergence of pen-on-paper (PoP) electronics, in which pens filled with conducting silver ink have been employed to create devices such as interconnects for light emitting diodes and antennas on paper.[14] The PoP approach requires inks with specific flow characteristics under ambient conditions, *i.e.* it should readily flow during writing and it should not coagulate in the pen. It has been shown that the resulting feature size of the written lines depend on the pen speed and the physiochemical properties of the ink and paper.[15]

Gellan gum (GG) is a linear anionic polysaccharide produced from the bacterium *Pseudomonas elodea*.[16,17] It is composed of tetrasaccharide repeating units of glucose, glucuronic acid and rhamnose in a molar ratio of 2 : 1 : 1.[18] Aside from its widespread application in food and cosmetics, GG's unique suspending (dispersing), gelation and rheological properties have been used in the processing of conducting carbon fillers such as single-walled carbon nanotubes, multi-walled carbon nanotubes and graphene.[19–22]

Carbon nanofibres are a conducting carbon filler which are closely related to carbon nanotubes, both in their structure and in their properties.[23] A catalytic thermal chemical vapour deposition synthesis method (with the use of a floating catalyst) has facilitated large-scale production of vapour-grown carbon nanofibres (VGCNFs).[24] The structure of these VGCNFs is "cup-stacked", meaning their stacking morphology is one of truncated conical graphene layers around a large hollow core.[25] Their average diameter (100 nm) and average length (50 to 200 μm) can be tuned by precise control of the synthesis conditions[25] and are similar to multi-walled nanotubes (MWNTs) produced by catalytic chemical vapour deposition.[26] As-produced VGCNFs are often coated with layers of amorphous carbon which serves to reduce the electrical conductivity due to low crystallinity.[27] This amorphous layer can be removed by post-treatment of the fibres with heat, which increases crystallinity[28] and results in a double-layered nanofibre.[29] The VGCNFs used in this paper underwent a heat treatment at 1500 °C which resulted in a highly graphitised outer layer of the hollow carbon fibre.

Carbon nanofibres have potential applications as gas sensors,[30] electrostatic paint and electronic shielding for the automotive industry and as components in batteries.[28] VGCNFs have been dispersed into various polymers including polystyrene (PS),[30] polypropylene (PP)[27,28] and poly(methyl methacrylate) (PMMA)[31] using high-shear stirring methods. It has been shown that using a sonication bath followed by high-speed mechanical stirring is a better dispersion method for VGCNFs

[a]*Soft Materials Group, School of Chemistry, University of Wollongong, Wollongong, NSW 2522, Australia*

[b]*Intelligent Polymer Research Institute, ARC Centre of Excellence for Electromaterials Science, AIIM Facility, University of Wollongong, Wollongong, NSW, 2522, Australia. E-mail: panhuis@uow.edu.au*

† Electronic supplementary information (ESI) available: UV-visible-NIR spectroscopy, light microscopy and sonication expense values. See DOI: 10.1039/c3ra43743d

(in an epoxy) compared to dispersing in a solvent or surfactant.[32] The reported electrical conductivity values for these composite materials ranged from 0.01 S $cm^{-1}$ (PMMA composite, 10% w/w VGCNF) to 2 S $cm^{-1}$ (PP composite, 60% w/w VGCNF).[26,30,33]

In this paper, we describe a carbon nanofibre ink suitable for the direct writing of conducting networks using a pen-on-paper direct writing approach. The VGCNF dispersion is optimised in terms of maximum VGCNF loading fraction. It is demonstrated that written electrodes on papers have suitable electrical properties, *i.e.* they can be used to draw simple circuitry for connecting a light emitting diode (LED) to a battery power source.

## 2. Experimental

### 2.1 Preparation of dispersions

Low acyl gellan gum (GG, Gelzan, Lot # 1I1443A) was received as a gift from CP Kelco. Gellan gum solutions (0.5% w/v) were prepared by dissolving dry powder (0.5 g) in Milli-Q water (100 mL, ~80 °C, resistivity 18.2 MΩ cm), while stirring at ~800 r.p.m (IKA RW 20 digital) for 30 minutes. Homogeneous dispersions of vapour grown carbon nanofibres (Pyrograf Products, PR24-LHT, Batch info: PS 1345 Box 8, HT 170) in GG were prepared using probe sonication. All dispersions were subjected to sonolysis using a digital sonicator horn (Branson Digital Sonifier) with a power output of 6 W in pulse mode (0.5 s on/off) and a tapered microtip (Consonic, diameter 3.175 mm) placed 1 cm from the bottom of a glass vial (diameter 25 mm).

### 2.2 Preparation of free-standing films

Drop-cast films were prepared by evaporative casting of composite dispersions into the base of a cylindrical plastic Petri-dish (diameter ~5.5 cm) and dried under controlled ambient conditions (21 °C, 50% relative humidity, RH, using a temperature/humidity chamber (Thermoline Scientific TRH-150-SD) for 24 h). The films were then peeled off the substrate to yield uniform free-standing films.

### 2.3 Direct writing

Direct writing was carried out using a commercially available fountain (nib) pen (Parker Jotter, Officeworks) with a refillable cartridge. VGCNF–GG inks were prepared as follows; GG solutions (3 mg $mL^{-1}$) were sonicated for 4 min (power output of 6 W) prior to addition of VGCNFs (10 mg $mL^{-1}$), followed by a further 4 min (power output of 6 W) of sonolysis. High quality photo paper (Spilman, matte, 180 g $m^{-2}$) was used as the substrate. Multiple circuits were prepared on paper substrates using direct written electrodes to connect LEDs (Jaycar Electronics, Australia, 5 mm diameter, green light source, 3.5 V switch on voltage) with a power source (6 V battery) using copper tape (3M).

### 2.4 Characterisation techniques

The absorbance behaviour of dispersions (diluted to VGCNF concentration of 6.67 mg $mL^{-1}$) was obtained using UV-vis-NIR spectroscopy (Cary 500 UV-Vis-NIR spectrophotometer) with a 1 cm path length cuvette. The wavelength of 1000 nm was arbitrarily selected for analysis as it is in the wavelength range at which VGCNFs exhibit absorbance features, but GG does not. Small aliquots (20 μL) of the dispersion sample were removed at varying sonication times and analysed for the presence of aggregated carbon inhomogeneity using a Leica Z16 APO optical microscope (8× magnification).

The flow properties of composite inks were studied using an Anton Paar Physica MCR 301 Digital Rheometer with a cone and plate measuring system (49.972 mm diameter, 0.992° angle, 97 μm truncation) and a heat controlled sample stage (Julabo Compact Recirculating Cooler AWC 100). Viscosity was measured between 0.1 and 100 $s^{-1}$ shear rate at 21 °C.

The surface morphology of films and written electrodes containing VGCNFs were assessed using scanning electron microscopy (FESEM JEOL JSM 7500-FA) and optical profilometry (Veeco Wyko NT9000). In order to obtain cross-sectional SEMs of fountain pen lines, the paper substrate was cooled using liquid nitrogen and snapped across the track. The thickness of drop-cast films was determined using a digital micrometer (Mitutoyo IP 65).

Electrical resistance measurements were carried out as follows. Evaporatively cast films were cut into strips of 3 mm × 25 mm and contacted (top and bottom) with conducting copper tape (3M) and conducting silver paint (SPI). The electrodes prepared by direct writing were contacted using the conducting copper tape. Current ($I$)–voltage ($V$) characteristics were obtained by measuring current using a digital multimeter (Agilent 34410A) under a cycling potential applied by a waveform generator (Agilent 33220A) under controlled ambient conditions (21 °C, 50% RH). $I$–$V$ plots were evaluated as a function of sample length ($L$), and used to calculate total resistance ($R_T$) values. The conductivity ($\sigma$) and contact resistance ($R_C$) were calculated by straight line fitting of the $R_T$ *versus* $L$ data to:

$$R_T = (1/A_{cross}\sigma)L + R_C, \quad (1)$$

where $A_{cross}$ is the cross-sectional area and $1/(A_{cross}\sigma)$ represents the sample resistance ($R_S$).

### 2.5 Statistical treatment

The reported results are averages of the values obtained. Reported numerical errors and graphical error bars are given as ±1 standard deviation (SD). Data and outliers were rejected either when instrumental error was known to have occurred, or if data failed a $Q$-test with a confidence interval ≥95%.

## 3. Results and discussion

### 3.1 Optimisation of dispersions

Previous research established that there is a strong correlation between UV-visible absorbance intensity and carbon-based materials.[34] In this work, the ability of the biopolymer gellan gum (GG) to disperse VGCNFs was assessed using UV-vis-NIR spectroscopy and light microscopy. It is assumed that the VGCNFs are completely dispersed when the UV-vis-NIR

absorbance reaches a plateau coupled with the disappearance of visible aggregates.

Fig. S1 (see the ESI†) shows that a dispersion (volume 10 mL) containing 1 mg $mL^{-1}$ VGCNFs and 1 mg per mL GG can be assumed to have reached completion after 4 min of sonication, *i.e.* the UV-vis-NIR absorbance plateaus (Fig. S1A and B†) and the visible aggregates have disappeared (Fig. S1C–K†). The amount (or expense, $E_\$$) of sonic energy (power × sonication) required to disperse 10 mg VGCNFs in 10 mL of dispersion is 144 J $mg^{-1}$.

The VGCNF–GG dispersion system was optimised by establishing the minimum energy (expense, $E_\$$) required to completely disperse a given mass of VGCNFs. The optimum sonication time (and expense) was found to increase with GG concentration in the investigated range (0.25–1.5 mg $mL^{-1}$) at constant VGCNF concentration (1 mg $mL^{-1}$), see Fig. 1a and Table S1 (see the ESI†). It is well known that the viscosity of polymer solutions increases with increasing polymer concentration. As such, it is suggested that the increase in sonication time is related to the increase in viscosity which is likely to drive down VGCNF mobility, therefore requiring more sonolysis to completely disperse the VGCNFs.

It is clear that GG is efficient at dispersing VGCNFs, *i.e.* only 1 min ($E_\$ = 36 \pm 18$ J $mg^{-1}$) of sonication is needed to disperse 10 mg of VGCNF in 10 mL at a VGCNF–GG ratio of 10 : 2.5.

As expected, the input sonication energy required to reach the point of complete dispersion increased as the VGCNF concentration was increased from 1 mg $mL^{-1}$ to 20 mg $mL^{-1}$ (Fig. 1). It should be noted that it was not physically possible to incorporate more than 200 mg VGCNFs in 10 mL of GG solution. Hence, we were unable to establish the upper concentration limit of the VGCNF.

The VGCNF expense was found to exhibit a minimum of 14.4 ± 3.4 J $mg^{-1}$ for a VGCNF–GG dispersion with VGCNF concentration = 10 mg $mL^{-1}$ (GG concentration = 3 mg $mL^{-1}$), see Fig. 1C. It is not clear at present what the dependence of expense and VGCNF concentration should be. However, it is likely that this dependence is influenced by rheological percolation effects related to either the dispersant GG and/or the carbon materials.[35,36]

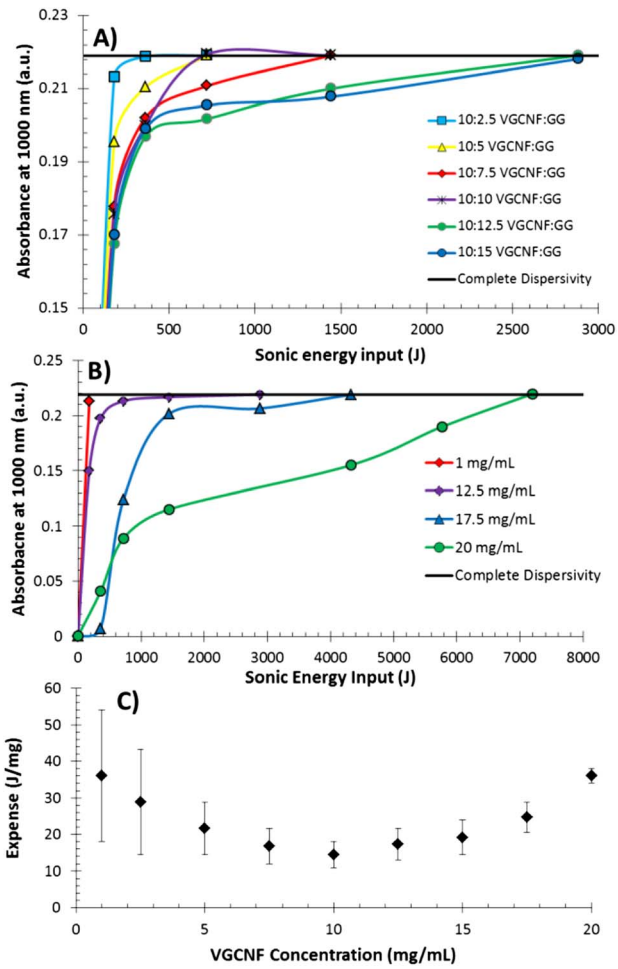


**Fig. 1** (A) UV-vis-NIR absorbance at 1000 nm as a function of sonication energy for 10 mg of VGCNFs dispersed in 10 mL GG solution at various VGCNF–GG ratios. The solid line indicates the expected absorbance for a complete dispersion. (B) UV-vis-NIR absorbance at 1000 nm *versus* input sonication energy for VGCNF–GG dispersions of increasing loading fraction. Horizontal black line represents the maximum absorbance for complete dispersion. (C) Expense to achieve a complete dispersion as a function of VGCNF concentration. All dispersions were diluted to a VGCNF concentration of 6.67 μg $mL^{-1}$.

### 3.2 Electrical characteristics of free-standing films

The electrical conductivity of freestanding VGCNF–GG films (mass ratio 10 : 3, mass fraction 0.77) prepared by evaporative casting was adversely affected by sonication. For example, the electrical conductivity of films prepared from a VGCNF–GG dispersion ($c_{VGCNF}$ = 5 mg $mL^{-1}$) subjected to 4 min of sonication is 35 ± 2 S $cm^{-1}$. As described above, increasing the VGCNFs loading requires longer sonication times, see Fig. 1B. For example, dispersing 20 mg $mL^{-1}$ of VGCNFs requires a sonication time of 20 min. The resulting films exhibited a lower conductivity (20 ± 2 S $cm^{-1}$) compared to films prepared using dispersions which were sonicated for 4 min, despite having the same VGCNF volume fraction. The decrease in conductivity was found to linearly decrease with increasing VGCNF concentration (Fig. 3A). We have attributed this to sonication-induced damage of the VGCNF, resulting in reducing the overall length. Similar effects have been previously reported for carbon nanotubes.[37–39]

The reduction in VGCNF length was examined using scanning electron microscopy (SEM) analysis (Fig. 2A and B). Length analysis (Fig. 2C) clearly indicates that the average length of the fibres is smaller for the dispersions sonicated for 20 min (average 1.1 μm) compared to 4 minutes (average 2.1 μm). Fig. 2C shows that the majority (60%) of the VGCNFs which had been sonicated for 20 min were between 0.5 and 1 μm in length. In contrast, the VGCNF dispersion which underwent 4 min of sonication consisted of VGCNFs with a wider range of lengths, including some with lengths of >3 μm. It is well-known that electrical transport through a network of conductors is determined by the number of junctions and the resistance of these junctions in the network.[40] The reduction in conductivity can then be argued as follows. VGCNF sonication

 

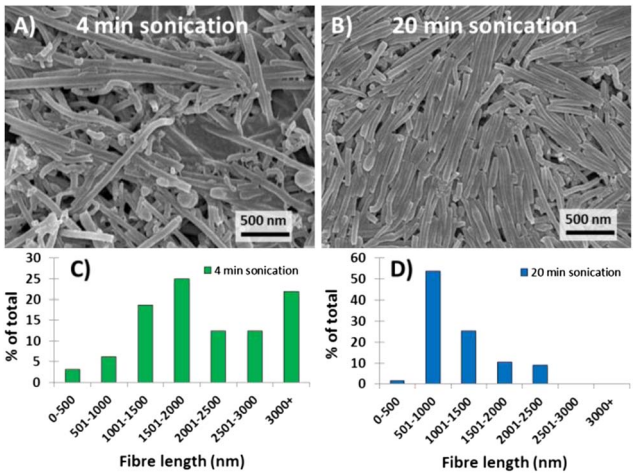


**Fig. 2** (A and B) SEM images of free-standing VGCNF–GG films (VGCNF volume fraction VGCNF = 0.69) prepared from VGCNF–GG dispersions (VGCNF concentration = 10 mg mL$^{-1}$, GG concentration = 3 mg mL$^{-1}$) which were sonicated for 4 minutes and 20 minutes, respectively. (C) and (D) Histograms showing length of the VGCNFs based on analysis of SEM images (28 μm$^2$ area) for samples sonicated for 4 and 20 minutes, respectively.

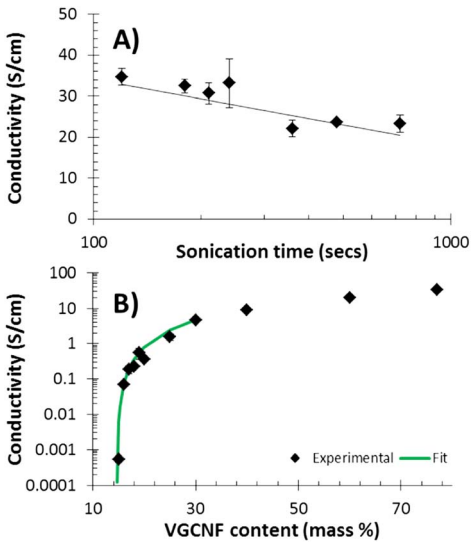


**Fig. 3** Electrical conductivity of drop cast films as a function of VGCNF (A) mass fraction and (B) sonication time. The solid line in (A) is a 3-parameter fit of the conductivity to the statistical percolation model, eqn (2). The straight line in (B) is a linear fit to the data.

results in a reduction in the length of the VGCNFs, which increases the number of junctions in the VGCNF network leading to an increased electrical resistance (decreased conductivity).

The percolation behaviour of the VGCNF–GG system was investigated by preparing free-standing films with different VGCNF loading fraction (Fig. 3B). The conductivity as a function of VGCNF mass fraction was fitted to the statistical percolation model:[41]

$$\sigma = \sigma_0(\varphi - \varphi_C)^t, \quad (2)$$

where $\sigma$, $\sigma_0$, $\varphi$, $\varphi_C$ and $t$ are the conductivity, scaling factor, mass fraction, mass fraction percolation threshold and the critical exponent, respectively. The fit predicted values for $\sigma_0$, $\varphi_C$ and $t$ as 0.046 ± 0.004 S cm$^{-1}$, 0.0147 ± 0.003 and 1.7 ± 0.2, respectively. The $t$ value is close to the theoretical predicted value ($t = 2.0$) for a 3D percolative network.[41]

### 3.3 Direct writing with a fountain pen

Direct writing was investigated using a commercial fountain (nib) pen. The flow curve of a typically used commercial ink (Parker "Quink" blue-black) is shown in Fig. 4, and was fitted to the well-known power law model,[42]

$$\eta = K\gamma^{n-1}, \quad (3)$$

where $\gamma$ is the shear rate, $K$ is the consistency index and $n$ is the power law index. This analysis revealed that the commercial ink exhibits near-Newtonian behaviour, *i.e.* $n = 0.9$. The viscosity of the commercial ink at shear rates common for pen writing (1000 s$^{-1}$) is approximately 0.81 mPa s. We achieved a similar viscosity (at this shear rate) by sonicating a gellan gum solution (3 mg mL$^{-1}$) for 4 minutes prior to adding 100 mg of VGCNFs and sonicating for a further 4 minutes.

Analysis of the flow curve of our VGCNF pen ink revealed consistency and power indices consistent with shear thinning behaviour, *i.e.* $K$ = 26 mPa s$^n$ and $n$ = 0.54, respectively. However, despite the rheological difference (near-Newtonian *vs.* shear thinning) our VGCNF ink has the required viscosity at the shear rates important for pen writing, *i.e.* $\eta = 1.1$ mPa s at shear rate = 1000 s$^{-1}$.

Lines were drawn (direct written) on a paper substrate using a fountain pen filled with our pen ink (VGCNF concentration = 10 mg mL$^{-1}$, GG concentration = 3 mg mL$^{-1}$ Fig. 5). The morphology of pen tracks on paper was investigated using optical and electron microscopy (Fig. 6). The characteristic "W" shape of nib fountain pen tracks is clearly visible in Fig. 6A and B.

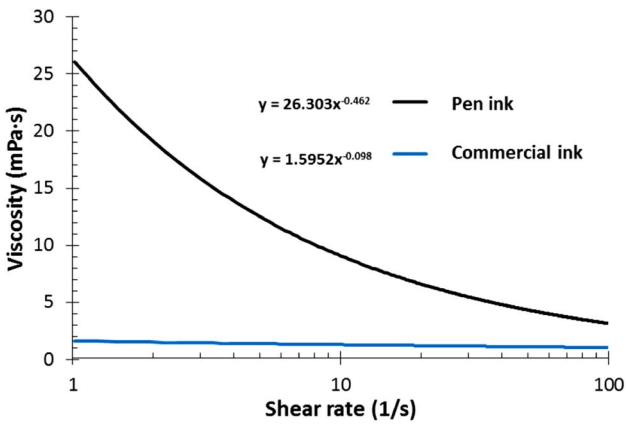


**Fig. 4** Viscosity as a function of shear rate for commercial pen ink (Parker "Quink" blue-black, dotted line) and VGCNF pen ink (solid line). The VGCNF ink was prepared by sonicating a gellan gum solution (3 mg mL$^{-1}$) for 4 minutes prior to adding 100 mg of VGCNFs (10 mg mL$^{-1}$) and sonicating for an additional 4 minutes.

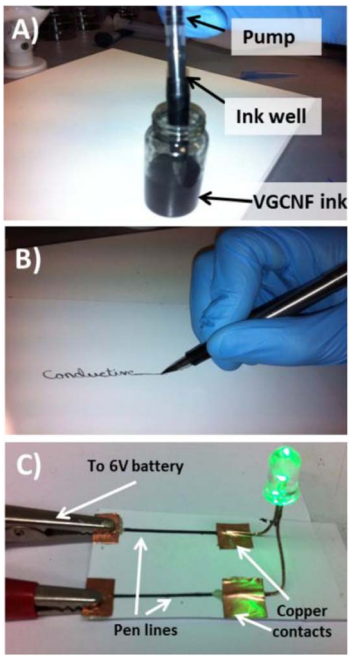


**Fig. 5** Direct writing of the VGCNF ink with a fountain pen. (A) Image of the commercial Parker Jotter fountain pen with pump-filled ink well and VGCNF ink, (B) image of the direct writing process, (C) Image of an LED powered by a power source (6 V battery) using direct written electrodes on a paper substrate (5 ink layers).

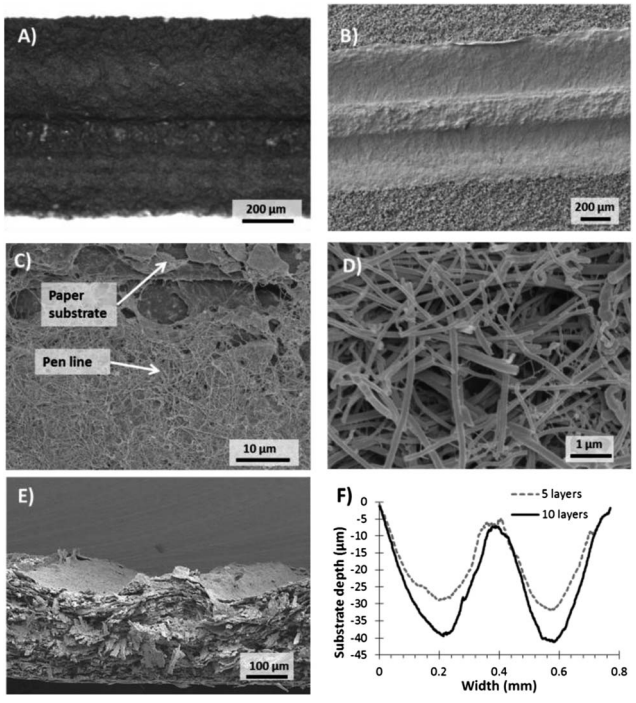


**Fig. 6** Morphology of typical direct written lines (electrodes, 5 layers) on the paper substrate. (A) Optical and (B) scanning electron microscopy (SEM) images of the line. (C) SEM image of the edge of a line. (D) Enlarged view of the VGCNF network. (E) SEM of the cross-section. (F) Optical profilometry of direct written lines (5 and 10 layers).

This shape is a result of the nib of the pen depressing the paper substrate during writing. Scanning electron microscopy (SEM) images revealed the presence of a VGCNF network in all areas of the "W" shape, including on the surface of the central ridge (Fig. 6C and D). Optical profilometry and cross-sectional SEM analysis was used to examine the effect of increasing the number of fountain pen ink layers on a paper substrate (Fig. 6F). It was found that increasing the number of pen layers resulted in a linear increase in the line width (Fig. 7A).

The number of layers had a significant effect on the electrical resistance (Fig. 7B). The resistance decreased by almost two orders of magnitude over 10 layers. The resistance (corrected for contact resistance) of the lines (channel length 5 cm) was found to have a power-law dependence on the number of pen layers according to:

$$R_S = R_{S1} L^P, \quad (4)$$

where $R_S$, $R_{S1}$, $L$ and $P$ are the sample resistance, sample resistance of 1 layer, number of layers and power-law index, respectively. Our fit revealed values of $R_{S1} = 75 \pm 1$ kΩ cm$^{-1}$ and $P = -1.218 \pm 0.006$. The fit underestimates the actual value for 1 direct written line ($97 \pm 20$ kΩ cm$^{-1}$), which is a likely to be a result of initial ink uptake by the paper substrate. The contact resistance $R_C$ also decreased with increasing number of pen layers (data not shown). These results indicate that with each written layer the amount of VGCNF deposited increases which leads to a better contact between sample and electrode, and an improved electrical resistance.[19]

The usefulness of our approach for direct writing paper electrodes for practical purposes was assessed by investigating the variability in the electrical resistance as a function of time for direct written lines, and the ability of electrodes to power an LED in a simple device. The variability was tested using two different approaches, (i) lines were direct written immediately

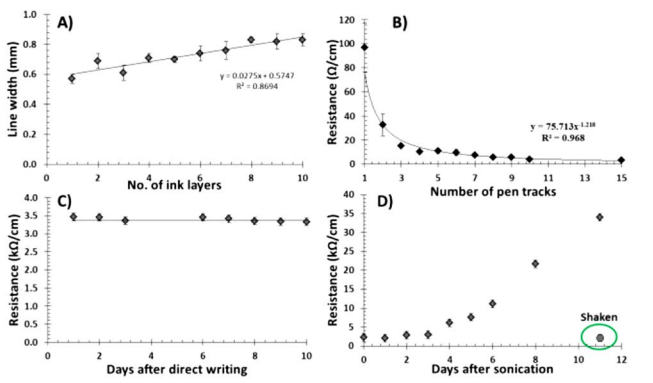


**Fig. 7** (A) Line width a function of number of ink layers for typical direct written lines on a paper substrate. Straight line is a linear fit to the data. (B) Electrical sample resistance of direct written lines as a function of number of ink layers on a paper substrate. Line is a power-law fit to the data. (C) Electrical (sample) resistance of typical direct written lines (10 layers) as a function of days after direct writing. Straight line is a guide to the reader's eye. (D) Electrical (sample) resistance of typical direct written lines (10 layers) as a function of resting time between ink preparation and direct writing. Circle indicates electrical resistance for an ink which was shaken on day 11 after preparation, prior to direct writing.

 

after ink preparation, and electrical testing was carried out as function of resting time (Fig. 7C), and (ii) there was a resting time between preparation of the ink and direct writing, followed by immediate electrical testing (Fig. 7D). It is clear that once processed, the electrical resistance ($3.4 \pm 0.1$ k$\Omega$ cm$^{-1}$) of the direct written pen lines (channel length 5 cm, 10 layers) does not change over 10 days. In contrast, the electrical resistance remains constant over the first 4 days, but then steadily increases with time between preparation of the ink and direct writing the electrodes. However, gentle shaking of the ink prior to direct writing can remove the increase in the electrical resistance (Fig. 7D). For example, shaking the ink after 11 days resulted in a reduced resistance, similar to that of the initial resistance values (within error). This suggests that the ink can be stored for up to 3 days prior to direct writing, while it will require gentle shaking for longer time periods to re-disperse the VGCNFs in the ink.

VGCNF written electrodes on paper were used in a simple circuit to connect an LED to a 6 V power source (Fig. 5C and D). Current–voltage measurements were taken across each of the written lines ($R_1$ and $R_2$, Fig. 5C) and across the LEDs. The average resistances across the 5-layered lines, $R_1$ and $R_2$, were found to be similar, *i.e.* $8.0 \pm 0.3$ and $8.0 \pm 1.1$ k$\Omega$ cm$^{-1}$, respectively. These measurements show that electrodes prepared by direct writing are stable over time and can be used in simple devices.

## 4. Conclusions

The dispersion optimisation of vapour-grown carbon nanofibres in solutions of the biopolymer gellan gum has been investigated. It was found that dispersing VGCNF in gellan gum required only short sonication times and low sonication energy input. For example, 1 mg mL$^{-1}$ of VGCNF could be completely dispersed in 1 mg mL$^{-1}$ gellan gum with 1 min of sonication at low power (6 W). It was demonstrated that gellan gum could easily disperse up to 20 mg mL$^{-1}$ of VGCNF at a VGCNG–GG ratio of 10 : 3, which required 20 min of sonolysis. The electrical conductivity of free-standing films decreased with increasing sonication time. For example, increasing the sonication time from 4 to 20 min decreased from 35 S cm$^{-1}$ to 20 S cm$^{-1}$, which was attributed to the observed sonication-induced damaged in the length of the conducting carbon filler.

Direct writing of VGCNF dispersions with a commercial fountain pen was also explored. The sonolysis protocol was changed to achieve VGCNF dispersion with similar viscosity at shear rates common to pen writing as a commercial pen ink. The electrical resistance of direct written electrodes on paper exhibited a power law dependence on the number of pen layers. Microscopy analysis suggested that with each successive pen stroke the amount of VGCNF increases leading to the observed improved electrical characteristics.

It was demonstrated that our direct written electrodes on paper can be used in simple device applications, such as connecting an LED to a power source. The electrical resistance of the paper electrodes was found to be stable for up to at least 10 days under ambient conditions. This paper contributes to the development of paper-based electrode materials.

## Acknowledgements

This work was supported by the University of Wollongong and the Australian Research Council (Centre of Excellence and Future Fellowship programs). The authors acknowledge use of the facilities and the assistance of Mr T. Romeo at the UOW Electron Microscopy Centre. Prof P. Calvert (University of Massachusetts) and Dr R Clark (CP Kelco) are thanked for stimulating discussions and provision of gellan gum, respectively.

## References

1 R. A. Giordano, B. M. Wu, S. W. Borland, L. G. Cima, E. M. Sachs and M. J. Cima, *J. Biomater. Sci., Polym. Ed.*, 1996, **8**, 63–75.
2 J. Beaman, H. Marcus, J. Barlow, M. Agarwala and D. Bourell, *Rapid Prototyping Journal*, 1995, **1**, 26–36.
3 G. Susanna, L. Salamandra, T. M. Brown, A. Di Carlo, F. Brunetti and A. Reale, *Sol. Energy Mater. Sol. Cells*, 2011, **95**, 1775–1778.
4 R. D. Piner, J. Zhu, F. Xu, S. Hong and C. A. Mirkin, *Science*, 1999, **283**, 661–663.
5 F. C. Krebs, *Sol. Energy Mater. Sol. Cells*, 2009, **93**, 465–475.
6 M. M. Voigt, R. C. I. Mackenzie, S. P. King, C. P. Yau, P. Atienzar, J. Dane, P. E. Keivanidis, I. Zadrazil, D. D. C. Bradley and J. Nelson, *Sol. Energy Mater. Sol. Cells*, 2012, **105**, 77–85.
7 J. Song, J. Kim, Y. Yoon, B. Choi, J. Kim and C. Han, *Nanotechnology*, 2008, **19**, 1–6.
8 T. H. J. van Osch, J. Perelaer, A. W. M. de Laat and U. S. Schubert, *Adv. Mater.*, 2008, **20**, 343–345.
9 B. J. de Gans, P. C. Duineveld and U. S. Schubert, *Adv. Mater.*, 2004, **16**, 203–213.
10 C. J. Ferris, K. G. Gilmore, G. G. Wallace and M. in het Panhuis, *Appl. Microbiol. Biotechnol.*, 2013, **97**, 4243–4258.
11 Z. Nie, C. A. Nijhuis, J. Gong, X. Chen, A. Kumachev, A. W. Martinez, M. Narovlyansky and G. M. Whitesides, *Lab Chip*, 2010, **10**, 477–483.
12 A. C. Siegel, S. T. Phillips, M. D. Dickey, N. Lu, Z. Suo and G. M. Whitesides, *Adv. Funct. Mater.*, 2010, **20**, 28–35.
13 G. P. Rolland and D. A. Mourey, *MRS Bulletin*, 2013, **38**, 299–334.
14 A. Russo, B. Y. Ahn, J. J. Adams, E. B. Duoss, J. T. Bernhard and J. A. Lewis, *Adv. Mater.*, 2011, **23**, 3426–3430.
15 J. Kim, M.-W. Moon, K.-R. Lee, L. Mahadevan and H.-Y. Kim, *Phys. Rev. Lett.*, 2011, **107**, 264501–264504.
16 E. R. Morris, K. Nishinari and M. Rinaudo, *Food Hydrocolloids*, 2012, **28**, 373–411.
17 T. J. Pollock, *J. Gen. Microbiol.*, 1993, **139**, 1939–1945.
18 P.-E. Jansson, B. Lindberg and P. A. Sandford, *Carbohydr. Res.*, 1983, **124**, 135–139.
19 N. Songmee, P. Singjai and M. in het Panhuis, *Nanoscale*, 2010, **2**, 1740–1745.

20 J. Boge, L. J. Sweetman, M. in het Panhuis and S. F. Ralph, *J. Mater. Chem.*, 2009, **19**, 9131–9140.
21 N. J. Whiteside, G. G. Wallace and M. in het Panhuis, *Synth. Met.*, 2013, **168**, 36–42.
22 L. Lu and W. Chen, *ACS Nano*, 2010, **4**, 1042–1048.
23 M. S. Dresselhaus, G. Dresselhaus and P. C. Eklund, *Science of fullerenes and carbon nanotubes: their properties and applications*, 1996.
24 G. G. Tibbetts, D. W. Gorkiewicz and R. L. Alig, *Carbon*, 1993, **31**, 809–814.
25 M. Endo, Y. A. Kim, T. Hayashi, Y. Fukai and K. Oshida, *Appl. Phys. Lett.*, 2002, **80**, 1267–1269.
26 N. Grobert, *Mater. Today*, 2007, **10**, 28–35.
27 M. Endo, Y. A. Kim, T. Hayashi, K. Nishimura, T. Matusita and K. Miyashita, *Carbon*, 2001, **39**, 1287–1297.
28 M. H. Al-Saleh and U. Sundararaj, *Carbon*, 2009, **47**, 2–22.
29 T. Uchida, D. P. Anderson, M. L. Minus and S. Kumar, *J. Mater. Sci.*, 2006, **41**, 5851–5856.
30 B. Zhang, R. Fu, M. Zhang, X. Dong, L. Wang and C. U. Pittman, *Mater. Res. Bull.*, 2006, **41**, 553–562.
31 G. A. Jimenez and S. C. Jana, *Composites, Part A*, 2007, **38**, 983–993.
32 S. Rana, R. Alagirusamy and M. Joshi, *J. Compos. Mater.*, 2011, **45**, 2247–2256.
33 K. Lozano, J. Bonilla-Rios and E. V. Barrera, *J. Appl. Polym. Sci.*, 2001, **80**, 1162–1172.
34 J. Yu, N. Grossiord, C. E. Koning and J. Loos, *Carbon*, 2007, **45**, 618–623.
35 G. C. Pidcock and M. in het Panhuis, *Adv. Funct. Mater.*, 2012, **22**, 4790–4800.
36 Y. Huang, S. Ahir and E. Terentjev, *Phys. Rev. B: Condens. Matter Mater. Phys.*, 2006, **73**, 1–9.
37 Q. Cheng, S. Debnath, E. Gregan and H. J. Byrne, *J. Phys. Chem. C*, 2010, **114**, 8821–8827.
38 P. Vichchulada, M. A. Cauble, E. A. Abdi, E. I. Obi, Q. Zhang and M. D. Lay, *J. Phys. Chem. C*, 2010, 12490–12495.
39 K. L. Lu, R. M. Lago, Y. K. Chen, M. Green, P. Harris and S. C. Tsang, *Carbon*, 1996, **34**, 814–816.
40 P. N. Nirmalraj, P. E. Lyons, S. De, J. N. Coleman and J. J. Boland, *Nano Lett.*, 2009, **9**, 3890–3895.
41 D. Stauffer and A. Aharony, *Introduction to Percolation Theory*, Taylor & Francis, London, 2nd edn, 1991.
42 J. A. Sánchez Pérez, E. M. Rodríguez Porcel, J. L. Casas López, J. M. Fernández Sevilla and Y. Chisti, *Chem. Eng. J.*, 2006, **124**, 1–5.

 